Earth and Planetary Science Letters, 345–361
Elsevier Science Publishers B.V., Amsterdam – Printed in The Netherlands

[6]

On the interaction between convection and crystallization in cooling magma chambers

Geneviève Brandeis and Claude Jaupart

Laboratoire de Géochimie et Cosmochimie, Université Paris 6 et 7, 4, place Jussieu, 75230 Paris Cédex 05 (France)

Received July 9, 1985; revised version received January 27, 1986

We investigate the interaction of thermal convection and crystallization in large aspect-ratio magma chambers. Because nucleation requires a finite amount of undercooling, crystallization is not instantaneous. For typical values of the rates of nucleation and crystal growth, the characteristic time-scale of crystallization is about 10^3–10^4 s. Roof convection is characterized by the quasi-periodic formation and instability of a cold boundary layer. Its characteristic time-scale depends on viscosity and ranges from about 10^2 s for basaltic magmas to about 10^7 s for granitic magmas. Hence, depending on magma viscosity, convective instability occurs at different stages of crystallization. A single non-dimensional number is defined to characterize the different modes of interaction between convection and crystallization.

Using realistic functions for the rates of nucleation and crystal growth, we integrate numerically the heat equation until the onset of convective instability. We determine both temperature and crystal content in the thermal boundary layer. Crystallization leads to a dramatic increase of viscosity which acts to stabilize part of the boundary layer against instability. We compute the effective temperature contrast driving thermal convection and show that it varies as a function of magma viscosity and hence composition.

In magmas with viscosities higher than 10^5 poise, the temperature contrast driving convection is very small, hence thermal convection is weak. In low-viscosity magmas, convective breakdown occurs before the completion of crystallization, and involves partially crystallized magma. The convective regime is thus characterized by descending crystal-bearing plumes, and bottom crystallization proceeds both by in-situ nucleation and deposition from the plumes. We suggest that this is the origin of intermittent layering, a form of rhythmic layering described in the Skaergaard and other complexes. We show that this regime occurs in basic magmas only at temperatures close to the liquidus and never occurs in viscous magmas. This may explain why intermittent layering is observed only in a few specific cases.

1. Introduction

Large igneous intrusions exhibit complex layered structures which have been recently reviewed by Irvine [1]. Their bewildering variety shows that many different processes operate in cooling magma chambers. What is widely recognized is that they are due to the combined effects of convection and crystallization [2–5]. There are now several competing models [2,6–8], and it is difficult to decide which applies where. It seems that no single physical framework can allow the interpretation of all structures, which presents an obvious difficulty for theoretical developments. The difficulty stems primarily from the impossibility of reproducing a magma chamber in the laboratory, due to a lack of comprehensive scaling analysis encompassing the effects of both convection and crystallization. Crystallization is a rate process determined by the kinetics of nucleation and crystal growth, and hence depends on the system considered.

It is clear that many processes can operate in magma chambers because several phases are involved (gas, crystals, liquid). Starting from a homogeneous liquid, all these complexities arise because of crystallization. The aim of this paper is to clarify which crystallization regimes are possible. We limit ourselves to the study of free convection. For the sake of clarity, two categories of free convection can be defined according to the driving mechanism. One is compositional convection driven by density contrasts due to fractional crystallization, suggested by Morse [9] and studied extensively by Huppert, Turner and Sparks [2,10–12]. The other is thermal convection driven

0012-821X/86/$03.50

by temperature contrasts. In a magma chamber, both play a role but it is not clear how: the thermal evolution of the chamber determines how crystallization proceeds, which in turn determines how composition and temperature evolve. In this paper, we study the limit case of thermal convection driven by cooling at a roof. This allows an understanding of the effects of the crystallization kinetics which differ between silicate liquids and the aqueous solutions used in the laboratory experiments of Huppert, Sparks and Turner [10–12]. The problem may be summarized as follows. As magma cools, its density increases and this makes it prone to convective instability. At the same time, it crystallizes and this acts to increase its viscosity and to stabilize it against convective instability. Were crystallization instantaneous, cold magma would behave rigidly and convection would only develop in regions above the liquidus. However, crystallization is not instantaneous and magma may become convectively unstable before crystallizing. We shall use recent results on thermal convection in fluids of variable viscosity to specify how this occurs. This will also allow a detailed model of the upper boundary layer and of the transition between the crystallizing upper border zone and the convecting interior of the chamber.

The plan of this paper is the following. We first set up a simple physical model of thermal convection. We start from basic physical principles and a limited set of parameters, and investigate systematically their range of variation. Section 3 is devoted to the governing equations and to a dimensional analysis which allows an easy understanding of the coupled effects of all parameters involved. In section 4, we present detailed numerical results and then discuss their validity with regard to the simplifying assumptions made. In a last section, we apply our results to real magma chambers and evaluate possible implications for the origin of igneous layering.

2. Thermal convection in magmas

We now consider a simple model of thermal convection. We focus our attention on reservoirs with large aspect-ratios, where the effects of side-wall cooling can be neglected (Fig. 1). This applies to basic complexes such as the Stillwater and the Bushveld, but also to any chamber towards the end of crystallization. Crystallization occurs mainly at the floor [5,9,13,14], hence the chamber gradually "fills up" and arrives at a stage where the effective aspect-ratio of the convecting reservoir is large.

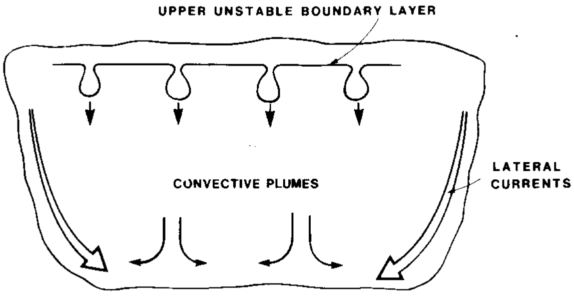

Fig. 1. Schematic representation of thermal convection in a magma chamber. There are two types of convective currents. Plumes are generated at the roof, and convective currents at the side walls. In this paper, we focus our analysis on large-aspect ratio reservoirs where the effects of side walls are small in the center.

Consider first a homogeneous liquid and neglect crystallization. Thermal convection is conveniently characterized by a single parameter, the Rayleigh number defined as follows:

$$Ra = \frac{\rho g \alpha \Delta T d^3}{\kappa \mu} \tag{1}$$

where κ is thermal diffusivity, μ dynamic viscosity, α the thermal expansion coefficient, ρ a reference density and g the acceleration of gravity. d is the chamber thickness and ΔT the driving temperature difference (i.e. the thermal contrast between roof and liquid magma). Typical values for these parameters are given in Table 1. As stressed by Shaw [3] and Bartlett [4], Ra is always very large, even for small values of ΔT. Hence, convection occurs in a turbulent regime [15], with a well-mixed interior and thin boundary layers at the top and bottom (Fig. 2). The important point is that fluid motions are not organized in a regular pattern of cells but in the form of downgoing plumes (Fig. 3). There are no rising plumes and the upward motions are diffuse. Finally, fluid dynamical experiments have shown the existence of a stagnant layer at the bottom of the reservoir [16].

At the top boundary, thermal convection is characterized by the quasi-periodic destruction of

TABLE 1

Definition and values of the parameters

Symbol	Quantity	Value
L	latent heat value	3.5×10^5 J kg^{-1}
c_p	specific heat	10^3 J kg^{-1} °C^{-1}
κ	thermal diffusivity	7×10^{-7} m^2 s^{-1}
ρ	density	2.8×10^3 kg m^{-3}
α	thermal expansion	5×10^{-5} °C^{-1}
g	gravity	10 m s^{-2}
I_m	maximum nucleation rate	7×10^6 m^{-3} s^{-1}
Y_m	maximum growth rate	6×10^{-8} m s^{-1}
δT	delay of nucleation	$\simeq 5$°C
E_0	activation energy above the liquidus	2.1×10^5 J mol^{-1}
E_1	activation energy below the liquidus	1.2×10^6 J mol^{-1}
μ_0	dynamic viscosity at the liquidus	
ν	kinematic viscosity	
T_u	temperature at the top of the unstable boundary layer	
T_L	liquidus temperature	
T_i	initial magma temperature	
ΔT	temperature contrast between country rock and magma	
ϕ	crystal content per unit volume	

the thermal boundary layer [17]. This boundary layer grows by conductive cooling until it becomes unstable (for example, see the photographs in Jaupart et al. [16]). Convective plumes appear and exhaust the boundary layer, which then reforms until the next instability. The instability occurs when a Rayleigh number defined locally exceeds a critical value [17]:

$$R_l = \frac{\rho g \alpha \Delta T \delta_c^3}{\kappa \mu} = R_c \qquad (2)$$

where δ_c is the boundary layer thickness. R_c is the critical value, about 200 within a factor of two depending on the boundary conditions [18]. As heat transfer is by conduction until convective breakdown, the critical time t_c is such that:

$$t_c \approx \frac{\delta_c^2}{\kappa} \qquad (3)$$

t_c defines the characteristic time-scale of thermal convection. Expressing (2) as a function of t_c instead of δ_c shows that the critical time increases with viscosity. Viscosity varies markedly among magmas, from values as low as 10 poise for ultramafic liquids up to values as high as 10^8 poise for rhyolite [19, p. 22]. This range translates into a large variation of critical times, whatever the value of ΔT. For example, an arbitrary value of 50°C for ΔT leads to values of t_c from 10^2 s to 10^7 s. These estimates must be compared to the time taken for crystallization. Using known rates of nucleation and crystal growth, we have shown that the characteristic time for crystallization is between 10^3 and 10^4 s [20]. This is bracketed by the range of critical times for the arbitrary ΔT of 50°C. When convective instabilities occur, crystallization is just starting in low-viscosity magmas, whereas it is fully developed in viscous ones. This shows that crystallization cannot be neglected and that this simple analysis is not valid. We now examine numerically a model poblem with crystallization and cooling in transient conditions.

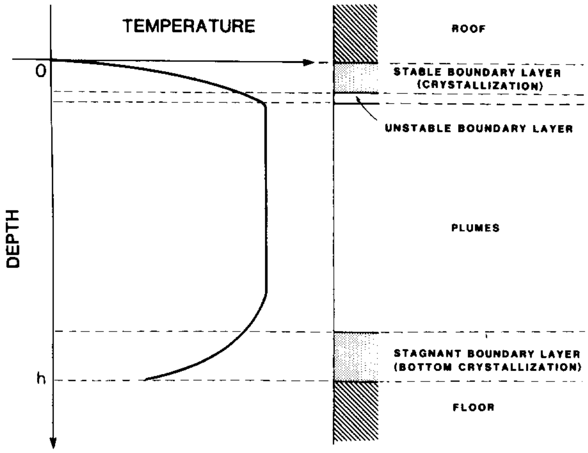

Fig. 2. Schematic representation of the temperature structure of thermal convection. In the middle, fluid is well-mixed and has a uniform temperature. Convective plumes are generated at the upper boundary layer. The chamber bottom is stagnant [16].

3. Convective instability during cooling and crystallization

We consider the simplest cooling experiment, in one dimension only (the vertical). At time $t = 0$, magma is emplaced in cold country rocks. As discussed earlier, thermal convection is characterized by the quasi-periodic breakdown of a boundary layer which grows by conduction. Hence, the problem is reduced to one of conduction until

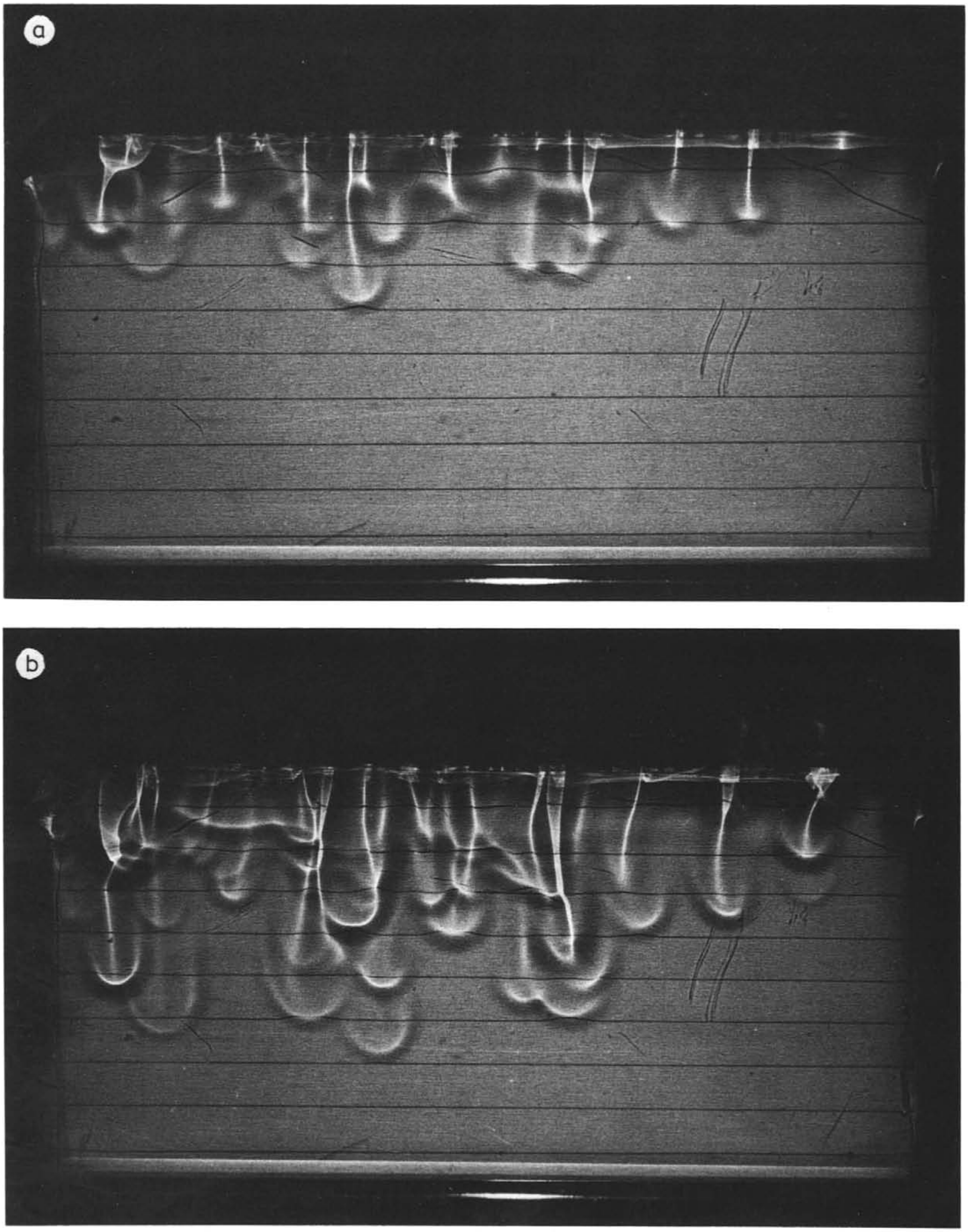

Fig. 3. Photographs of developing thermal convection (from [16]). At the top boundary, cooling generates cold plumes which move downwards.

the onset of instability. We assume that crystallization takes place in magma only. The heat equation is written:

$$\partial T/\partial t = \kappa \partial^2 T/\partial z^2 \quad \text{for } z < 0 \text{ (country rock)} \qquad (4a)$$

$$\partial T/\partial t = \kappa \partial^2 T/\partial z^2 + L/c_p \, \partial\phi/\partial t \quad \text{for } z > 0 \text{ (magma)} \qquad (4b)$$

where c_p is the isobaric heat capacity and L the latent heat per unit mass. ϕ is the crystal content per unit volume and takes values between 0 and 1. $\partial\phi/\partial t$ depends on the nucleation and growth rates according to the equation [21]:

$$\partial\phi/\partial t = 4\pi(1-\phi)Y(t)\int_0^t I(v)\left[\int_v^t Y(u)\,\mathrm{d}u\right]^2 \mathrm{d}v \qquad (5)$$

I and Y are the rates of nucleation and growth which depend on temperature according to expressions given in Appendix A. These expressions have been determined using simple non-equilibrium thermodynamics and the results of laboratory experiments. The initial conditions are that both magma and country rock are initially isothermal, with an initial temperature contrast ΔT:

$$T(z, 0) = T_i \quad \text{for } z > 0 \text{ (magma)} \qquad (6a)$$

$$T(z, 0) = T_i - \Delta T \quad \text{for } z < 0 \text{ (country rocks)} \qquad (6b)$$

T_i denotes the initial magma temperature. At $t = 0$, the contact temperature is instantaneously carried to $(T_i - \Delta T/2)$, and then increases as crystallization proceeds (see [20]). Hence the thermal contrast decreases.

The equations of T and ϕ are coupled. To understand the effects of all parameters, it is useful to write down the equations in dimensionless form. To this aim, we first assume that the physical properties are constant. The temperature scale is ΔT, and both a depth-scale and a time-scale are needed. In this problem, the depth-scale is the boundary layer thickness, which is also defined as the convective depth-scale [15]:

$$\delta_c = \left(\frac{g\alpha\Delta T}{R_c \kappa \nu}\right)^{-1/3} \qquad (7a)$$

ν is kinematic viscosity, i.e. μ/ρ. Because heat transfer is by conduction, the corresponding time-scale is simply the critical time already defined above:

$$t_c = \frac{\delta_c^2}{\kappa} \qquad (7b)$$

The obvious scales for the nucleation and growth rates are the maximum values I_m and Y_m (see Appendix A). The non-dimensional variables are denoted by primes:

$$t = t' t_c \qquad (8a)$$

$$z = z' \delta_c \qquad (8b)$$

$$I = I' I_m \qquad (8c)$$

$$Y = Y' Y_m \qquad (8d)$$

$$T = T_i + T' \Delta T \qquad (8e)$$

The system of equations (4) to (5) becomes, dropping the primes:

$$\partial T/\partial t = \partial^2 T/\partial z^2 \qquad (9a)$$

$$\partial T/\partial t = \partial^2 T/\partial z^2 + L/(c_p \Delta T)\partial\phi/\partial t \qquad (9b)$$

$$\partial\phi/\partial t = t_c^4 (Y_m^3 I_m) 4\pi(1-\phi)Y(t)\int_0^t I(v) \times \left[\int_v^t Y(u)\,\mathrm{d}u\right]^2 \mathrm{d}v \qquad (9c)$$

This introduces two characteristic numbers, the Stefan number σ, and a new number denoted by C:

$$\sigma = \frac{L}{c_p \Delta T} \qquad (10a)$$

$$C = \frac{1}{\kappa^4}\left(\frac{R_c \kappa \nu}{g\alpha\Delta T}\right)^{8/3} (Y_m^3 I_m) \qquad (10b)$$

The Stefan number gives a measure of the importance of latent heat in the temperature equation. If it is small ($\sigma \ll 1$), then crystallization can be neglected in the heat budget. For the parameter range of interest here, as in most geological problems, the Stefan number is close to 1, thus latent heat release is a significant process. The number C can be rewritten as:

$$C = \left(\frac{t_c}{\tau_c}\right)^4 \qquad (11a)$$

where τ_c has the dimension of time and is defined as:

$$\tau_c = (Y_m^3 I_m)^{-1/4} \qquad (11b)$$

τ_c is the characteristic time for crystallization. With the numerical values used here (Table 1), it is 5×10^3 s. Equation (11a) shows that C is the ratio between the time-scales for convection and crystallization. From equation (9c), if C is small ($C \ll 1$), then $\partial\phi/\partial t$ is also small, hence crystallization is not significant when convection develops. If, on the other hand, C is large ($C \gg 1$), then crystallization cannot be neglected.

From (10b), it is seen that C increases with magma viscosity, and also with the rates of growth and nucleation. In the following, we shall keep Y_m and I_m both constant for reasons detailed in Appendix A. Using these values, varying viscosity from 10 poise to 10^8 poise leads to values of C ranging from 4×10^{-9} to 2×10^{10}. Therefore, varying viscosity between the bounds for silicate liquids entails spanning the whole range of values for C, and hence the whole spectrum of possibilities for the interaction between crystallization and convection.

This non-dimensional analysis allows a quick glance at the problem. It is unfortunately oversimplified because all parameters vary dramatically in the boundary layer: temperature, crystal content, and hence viscosity [22,23]. Thus, there are no simple scales for all these variables, as explicitly assumed above. Furthermore, the vertical variation of viscosity becomes an important parameter [18], and there is no simple way to parameterize it since it changes with time. The same problem is encountered in mantle convection when allowance is made for the temperature dependence of viscosity, and a series of simple techniques are available to characterize instability [18,24].

We proceed as follows. Crystallizing magma is treated as a mixture of crystals and liquid. The conduction equations are integrated numerically using the method of our earlier paper [20]. We follow the evolution of temperature and crystal content and calculate the viscosity profile using the relationship defined in Appendix B. Because viscosity varies significantly, the whole boundary layer does not go unstable ([18] and Fig. 4). Only its lowermost part where viscosity is lowest does so, leaving the viscous top unaffected. The unstable part has thickness δ. The temperature at the interface between the stable and unstable parts is T_u (Fig. 4). This determines the effective driving temperature difference of convection, i.e. the thermal contrast between the chamber roof and convecting interior. To calculate the values of δ and T_u, we use the instability criterion developed by Jaupart and Parsons [18] which allows the treatment of fairly arbitrary viscosity variations. This criterion yields results similar to others and is in agreement with laboratory experiments [25,26] as well as numerical studies [27,28]. We compute a local Rayleigh number at any depth z in the magma where temperature is $T(z)$:

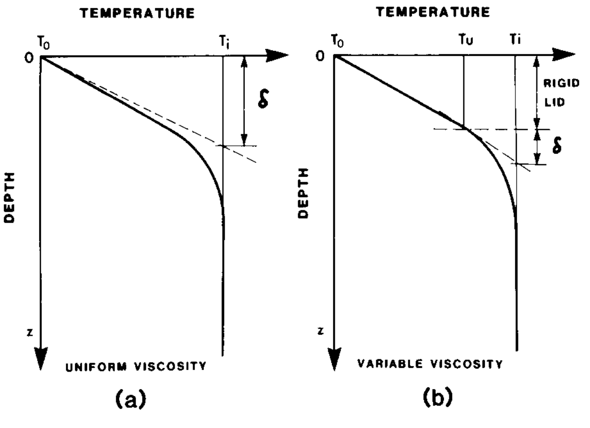

Fig. 4. Schematic profiles of temperature at top of the convecting chamber, illustrating the difference between uniform and variable viscosity. T_0 is the temperature at the upper border. The upper border is initially at the chamber roof and migrates downwards as crystallization proceeds. (a) Uniform viscosity. The top of the unstable boundary layer is at the upper border with temperature T_0. The broken line is the tangent to the temperature curve and shows how δ is defined (equation 13). (b) Variable viscosity (due to temperature and crystals). The upper part of the thermal boundary layer is highly viscous and behaves rigidly. Only the lower part of thickness δ is unstable. T_u, the temperature at the top of the unstable boundary layer, is higher than T_0.

$$Ra(z) = \frac{\rho g \alpha [T_i - T(z)][\delta(z)]^3}{\kappa \mu(z)} \tag{12}$$

$\mu(z)$ is viscosity at depth z and $[T_i - T(z)]$ is the local temperature contrast. $\delta(z)$ is a local depth-scale defined as:

$$\delta(z) = \frac{[T_i - T(z)]}{\dfrac{\partial T}{\partial z}(z)} \tag{13}$$

The local Rayleigh number defined by (12) depends on both depth and time. As shown in [18], at any given time, it has a bell-shaped profile, reaching a maximum in the boundary layer and decreasing to zero below. This profile evolves with time, with increasing values as cooling proceeds. This allows up to determine when and how convective breakdown occurs. Instability sets in when the maximum of $Ra(z)$ exceeds a critical value of 200. Also, the depth of the maximum defines the level separating the stable and unstable parts of the boundary layer. This allows us to define which part of the cold boundary layer remains stable because of its greater viscosity.

The parameters of the problems are: T_i, the initial magma temperature, ΔT, the initial temperature contrast between magma and country rocks, and μ_0, the viscosity at the liquidus.

We assume that T_i is equal to the liquidus T_L. We shall also consider the case where the initial temperature is slightly greater than the liquidus, i.e. magma is superheated. Superheating is the natural consequence of melt extraction from a partially molten source. The degree of superheating is a function of composition and of the vertical distance separating the source and the chamber. For a natural lherzolite source and a tholeiitic liquid, superheating may reach several tens of degrees [29, p. 411]. There is an additional reason why magma cannot be much below the liquidus. Supposing this is the case, we have shown in [20] that nucleation is so extensive that latent heat release brings it back to the liquidus. Dowty [30] reached the same conclusion, whatever the heat loss mechanism is, because heat transfer in geological conditions cannot evacuate the heat released by crystallization over a large volume. This is why thermal calculations always show that crystallization is limited to thin boundary layers. Campbell [31] gave field arguments which support this view. We shall investigate a range of initial temperatures from T_L to $T_L + 100°C$.

The initial temperature of country rocks is set at a fixed value ($T_L - 600°C$). Thus, ΔT is always larger than 600°C, corresponding to conditions of intrusion in cold country rock. As shown in [20], the contact temperature increases rapidly, hence the temperature contrast drops to small values. Even for these high initial temperature contrasts, the thermal evolution depends weakly on ΔT, hence there are in reality only two governing parameters: μ_0 and T_i.

4. Results

We illustrate our results as a function of two variables, T_i and μ_0. We determine at which stage of the crystallization sequence convective instability sets in. The idea is to proceed as in the non-dimensional analysis above. However, instead of just one characteristic time for crystallization, there are two. Crystallization proceeds both by nucleation and crystal growth. As discussed in our earlier paper [20], there is a nucleation delay, and hence nucleation does not start until some time t_1 [20]. We define the onset of crystallization at time t_1 such that the crystal content exceeds a critical value of 0.01% somewhere in the undercooled boundary layer. Once crystallization has started, it takes time to develop and is not completed anywhere until some time t_2. Time t_2 is such that the crystal content reaches 99% somewhere in the cooled boundary layer. Between times t_1 and t_2, the cooled boundary layer contains crystals, but is only partly crystallized. Times t_1 and t_2 play roles similar to τ_c defined in (11b). In fact, τ_c is found to lie between the two. The critical time t_c for convective instability depends on how crystallization proceeds (through the viscosity effect). Fig. 5

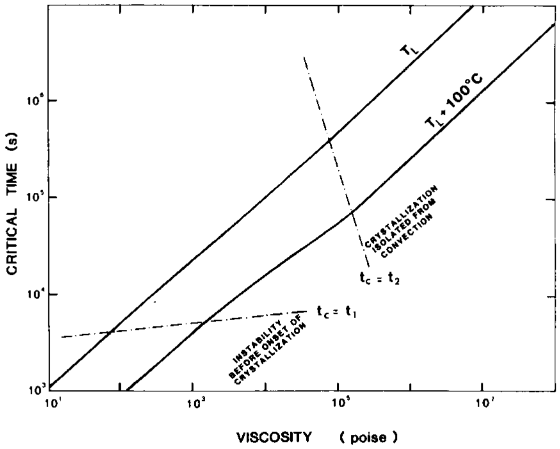

Fig. 5. Critical time for onset of convection (t_c) as a function of viscosity μ_0 (μ_0 is the value at the liquidus). Calculations for two values of the initial magma temperature are shown: T_L and ($T_L + 100°C$). There are three cases. For small viscosity values, t_c is lower than t_1: instability occurs before the onset of crystallization. For large viscosity values, t_c is larger than t_2 and crystallization develops faster than convection. For intermediate viscosity values t_c lies between t_1 and t_2: there is interaction between crystallization and convection.

shows plots of t_c as a function of μ_0 for two different values of T_i, the initial magma temperature. Note that the curves are similar and that t_c increases as μ_0 increases, spanning the whole crystallization sequence from times less than t_1 to times greater than t_2. We now examine in detail the various regimes of instability to specify the structure of the unstable boundary layer. We first fix T_i at the liquidus.

4.1. Initial magma temperature at the liquidus

Using the rates of nucleation and growth defined in Appendix A and in Table 1, t_1 is equal to 2×10^3 s. There are three different cases (Fig. 5).

Case a: $t_c < t_1$: $\mu_0 \leqslant 40$ poise (Fig. 6). The instability occurs before the onset of crystallization. There are very few crystals in the undercooled boundary layer (Fig. 6c). The viscosity variation is moderate (Fig. 6b) and mostly due to the temperature effect. T_u is below the liquidus: the temperature contrast across the unstable boundary layer can exceed values of 50°C (Fig. 6a). Note that it is considerably smaller than the initial contrast between country rocks and magma.

Case b: $t_1 < t_c < t_2$: $40 \leqslant \mu_0 \leqslant 10^5$ poise. Partly crystallized magma is taken up in the instability. The structure of the thermal boundary layer is the following. Between temperatures T_L and $(T_L - \delta T)$, where δT is the nucleation delay (see Appendix A), there are no crystals. At temperatures lower than $(T_L - \delta T)$, crystals are nucleated and grow, and the crystal content ϕ varies steeply. Viscosity also increases steeply and acts to stabilize the region where ϕ is greatest. T_u is somewhat lower than $(T_L - \delta T)$. This case is intermediate between case (a) above and case (c) below. As μ_0 increases, the critical time increases and crystallization has time to develop. With more crystals, viscosity increases and instability can only be at hotter levels. T_u increases with μ_0, eventually reaching the limit $(T_L - \delta T)$ when μ_0 equals 10^5 poise (Fig. 7).

Case c: $t_c > t_2$: $\mu_0 \geqslant 10^5$ poise (Fig. 8). Crystallization is fully developed, with a thin crystallization interval (a few centimeters) advancing as cooling proceeds. In the undercooled boundary layer, the viscosity increase is steep and the whole crystallization interval remains stable. T_u is equal to $(T_L - \delta T)$ and there are no crystals in the unstable boundary layer (Fig. 8a).

4.2. Initial magma temperature above the liquidus

We now suppose that magma is slightly superheated. In this case, there is a heat flux from the magma into the crystallizing region. Country rocks must evacuate both this and the heat released by crystallization, hence crystallization is slower. As

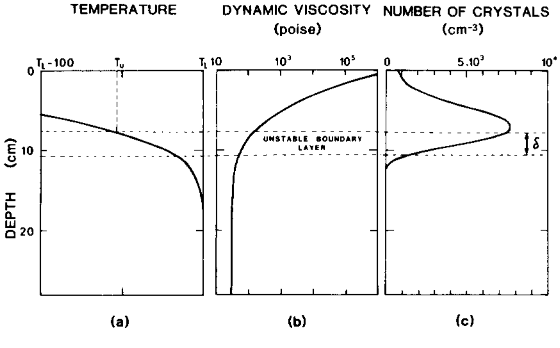

Fig. 6. Vertical profiles of temperature, viscosity and crystal content at time t_c for $\mu_0 = 30$ poise. This case is such that $t_c < t_1$, i.e. crystallization has not begun. $z = 0$ is at the contact with country rocks. The unstable boundary layer has thickness δ. Note that T_u is much lower than the liquidus and that there are few nuclei in the unstable boundary layer.

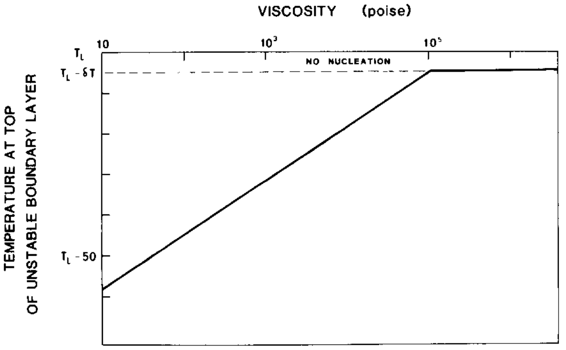

Fig. 7. Temperature at the top of the unstable boundary layer (T_u) versus viscosity for $T_i = T_L$. δT denotes the nucleation delay and is such that there are no nuclei between temperatures T_L and $T_L - \delta T$. For $\mu_0 < 10^5$ poise, T_u is smaller than $T_L - \delta T$ and the unstable boundary layer contains crystals. For $\mu_0 > 10^5$ poise, T_u is equal to $(T_L - \delta T)$ and there are no crystals in the unstable boundary layer.

stressed in [20], the main result is that the crystallization interval is thinner. Thus the viscosity increase in the boundary layer is steeper than before, which acts against convective instability [18].

This case is similar to the previous one, with t_c increasing as a function of μ_0 (Fig. 5). There is, however, a subtle effect. In magmas of low viscosity, convection sets in very early if T_i is high. Fig. 9 shows the evolution of T_u as a function of T_i for a viscosity of 30 poise. T_u increases with T_i, exceeding the liquidus when T_i exceeds (T_L + 70°C). In that case, convection develops only in the lowermost part of the boundary layer, where there are no crystals. This is the same situation as case (c) above. This shows that the interior temperature is an important parameter.

4.3. Summary

As shown in previous studies [18,24–26], the effect of variable viscosity is to reduce the strength of convection. The temperature difference which effectively drives convection is equal to $(T_i - T_u)$, hence it is much smaller than the total temperature difference. In the example of Fig. 8, the driving temperature contrast is only 5°C, compared to an initial contrast of 600°C between magma and country rocks. In Fig. 9, we compare two magmas with different viscosities. At low viscosity, T_u can be quite lower than $(T_L - \delta T)$, hence the driving temperature contrast is not negligible, exceeding several tens of degrees. At high viscosity, T_u remains equal to $(T_L - \delta T)$, hence the driving temperature contrast is always small. We conclude that viscous magmas are characterized by weak thermal convection, owing not only to their high viscosity, but also to the fact that the driving temperature contrast is small. This implies lower convection velocities and a different regime of thermal convection, with no transfer of crystals in the convecting magma.

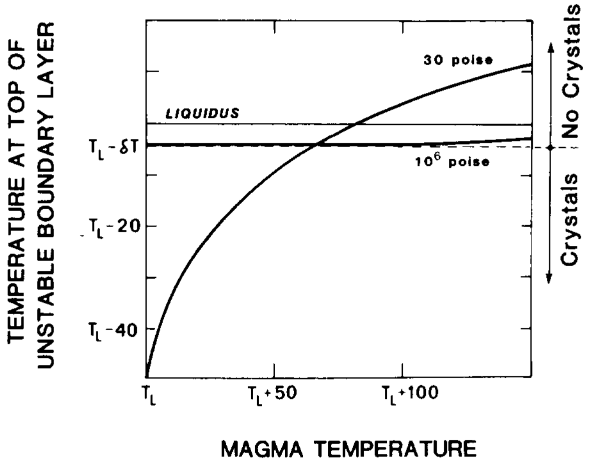

Fig. 9. Temperature at the top of the unstable boundary layer (T_u) versus initial magma temperature (T_i) for two viscosity values (30 and 10^6 poise). If T_u is lower than $(T_L - \delta T)$, there are crystals in the unstable boundary layer and hence in the convective plumes. The regime of crystal-bearing plumes applies to magmas with viscosities less than 10^5 poise and initial temperatures close to the liquidus.

As shown in Fig. 3, the breakdown of the unstable boundary layer generates convective plumes which travel downwards. As they reach the

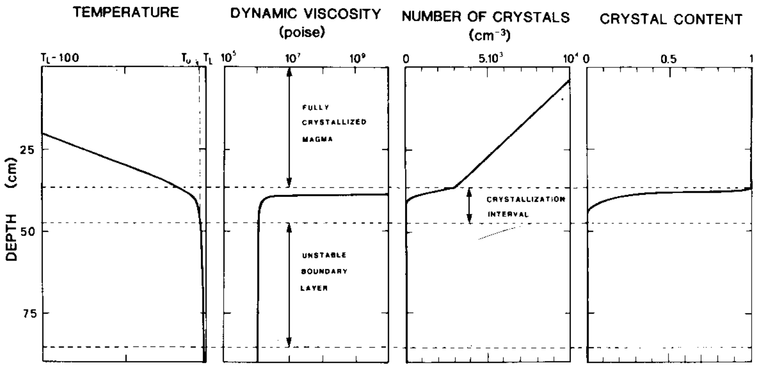

Fig. 8. Same as Fig. 6 for $\mu_0 = 10^6$ poise, corresponding to a large critical time ($t_c \geq t_2$). Crystallization is fully developed when convective breakdown occurs. Note the fully crystallized layer ($\phi = 1$) lying at the top. T_u is close to the liquidus, and there are no crystals in the unstable boundary layer.

chamber bottom, they will interact with the crystallization taking place there. We have described three cases, but we need only define two regimes. For comparison with petrological observations, it is important to distinguish between crystal-bearing plumes and crystal-free ones:

—Crystal-free plumes (case c). There are no crystals in the unstable boundary layer. This regime is the only one for viscous magmas and is possible in fluid magmas at high temperatures. Crystallization is limited to stable boundary layers which are isolated from the convecting part of the chamber.

—Crystal-bearing plumes (cases a and b). The unstable boundary layer contains crystals. This corresponds to viscosity values less than 10^5 poise and magma temperatures close to the liquidus. A form of convection similar to crystal-bearing plumes had been suggested by Hess [14] to explain some of his observations in the Stillwater complex. The contribution of this paper is to determine the parameter range in which this regime is possible.

One essential difference between the two regimes is the thermal state of the chamber interior. There, convection is turbulent with temperature fluctuations whose magnitude is given by the temperature difference across the unstable boundary layer. Again, the important point is that thermal convection occurs in the form of cold downgoing plumes with diffuse return flow. The temperature structure is not random and can be described as a set of cold regions (plumes) against a hotter background. In the first regime, temperatures inside the plumes remain close to the liquidus. In the second regime, they are below the liquidus.

4.4. Discussion

We have studied thermal convection which is a limit case as no account is taken of other effects such as crystal settling and compositional differences. This is not a problem for magmas of low viscosity since we have shown that convective instabilities develop faster than crystallization. Thus, when convective breakdown occurs, crystals have not yet reached large sizes, hence settling is not significant. For the same reason, compositional contrasts have not developed. Compositional effects develop mostly in the bottom boundary layer at a rate controlled by crystallization, i.e. on a larger time-scale than thermal convection at the top.

In magmas with viscosities greater than 10^5 poise, crystallization develops faster than convective instability. Therefore, thermal convection is weak and may be negligible compared to other processes such as crystal settling and compositional convection. A full evaluation of all possible processes is beyond the scope of this paper, but it is clear that thermal convection is not significant, with small temperature differences and small velocities.

Other effects are possible in magma chambers. For example, Morse [32] has developed a model of roof foundering in which already crystallized magma is detached and sinks. The effects of such crystal packets are not distinguishable from those of crystal-bearing plumes. Although the effects are similar, the physics are not. Our model depends on a limited set of parameters and allows the definition of different regimes and their parameter range. Hence, it provides a simple framework which is useful in explaining why the same features are not observed in all igneous complexes. It is also useful in sorting out those features which cannot be accounted for by the model, and thus in showing the need to incorporate other effects.

Our calculations depend on the viscosity function and on the rates of nucleation and growth. The activation energy for the viscosity of silicate liquids does not vary by more than a factor of 3, hence the results depend weakly on the particular value selected. The nucleation and growth functions determine the values of t_1 and t_2, the characteristic times for crystallization. Varying the crystallization parameters within measured bounds leads to variations of less than one order of magnitude ([20], see also Appendix A).

The physical experiment we used is simple and may seem valid only in early stages following emplacement. However, the argument of section 2 leads to similar numerical estimates for the critical time, which shows that it is not sensitive to the model chosen. For back-of-the-envelope estimates, the method of section 2 or the use of non-dimensional number C are sufficient. This indicates that the results are of more general value. As shown in [20], after a short transient stage of less than 10^3 s, the thermal regime depends weakly on the initial conditions and calculated temperatures in the undercooled boundary layer differ by less than 20°C. This shows that our results are not significantly affected by the value of ΔT since instability always sets in at times longer than this short transient (Fig. 5). Furthermore, as discussed in section 2, the effect of μ_0 is much more important than that of ΔT. Thus, considering a chamber in an evolved state, the convection regime can be evaluated using the temperature in the chamber interior instead of T_i. Because of the necessary simplifying assumptions, the numerical results must be taken as representative only, but it is clear that the characteristic times for convection and crystallization are similar for basic magmas, whereas they differ markedly for silicious ones. We examine in section 5 a few petrological implications.

5. Petrological implications

In basic or ultrabasic magmas, we suggest that there are two different regimes of thermal convection. If the interior temperature is greater than the liquidus by more than about 70°C, the convective plumes would not carry crystals. Therefore, in-situ crystallization at the floor would proceed without direct interference from the plumes (Figs. 2, 3 and 10a). In contrast, when the interior temperature is close to the liquidus, the convective plumes contain crystals (Fig. 10b). The fate of these crystals is complex. After being nucleated in the boundary layer, they are taken up in plumes where temperature fluctuations are large. They may either grow or be resorbed. This depends on the value of the interior temperature. For example, if it equals the liquidus, the whole temperature history of plumes is below the liquidus, hence there is no resorption.

For comparison with field observations, it is useful to estimate the size of plumes. There are many problems when applying theoretical considerations to natural cases [33, p. 230], but it is possible to obtain order of magnitude estimates. The plumes develop from disturbances in the boundary layer which have a characteristic wavelength λ proportional to its thickness. From laboratory experiments and numerical studies, one finds:

$$\lambda \approx 8\delta \qquad (14)$$

Thus, each plume draws fluid from a cylinder of diameter λ and height δ. This corresponds to a spherical cap (the starting plume) of diameter 5δ. This simple formula agrees with our laboratory observations. For the cases considered here (Figs. 6a and 8a), δ varies from about 5 to 30 cm depending on viscosity. For a representative value of 20 cm, the initial plume diameter is thus about 1 m.

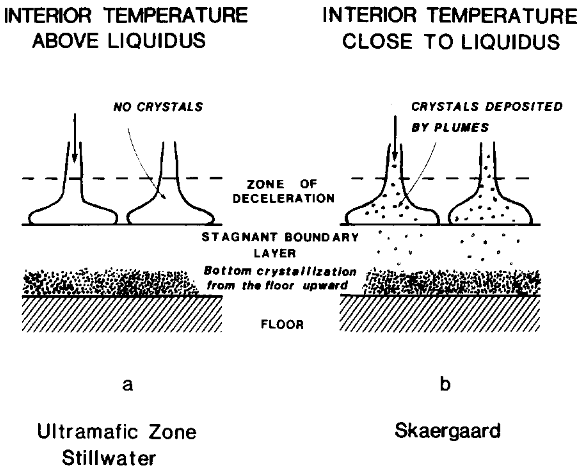

Fig. 10. Schematic representation of the two regimes of bottom crystallization in convecting magma. Convection occurs in the form of downgoing plumes. In reality, the plumes are turbulent and their boundaries are not as sharp as drawn here. In the first regime (a), the plumes do not carry crystals. We suggest that this regime prevailed during formation of the Ultramafic Zone of the Stillwater. In the second regime (b), the plumes carry crystals which are deposited at the bottom. We suggest this is the origin of intermittent layering, as observed in the Skaergaard.

These plumes first evolve in a regime dominated by viscosity and are therefore laminar, but they become turbulent at some distance from the boundary [15]. Turbulent plumes grow by entraining surrounding fluid [33, p. 167]. For free convection, the process of entrainment includes the mixing of one plume into another [33, p. 230], and the plume diameter b increases linearly with depth according to the formula:

$$b \approx (6/7)\alpha_e z \qquad (15)$$

α_e is the entrainment constant, which is about $(0.116/\sqrt{2})$ [33, p. 231]. For a chamber thickness of 1 km, say, the plume diameter is found to be 80 m when it reaches the bottom. This calculation is simplified, but shows that plumes can reach large sizes and thus have an effect over large horizontal distances.

Another point is that the flow field in a plume is complex, with both eddies and vertical mean motion (Fig. 11). As a plume impinges on the bottom boundary layer, it spreads laterally, slows down, and deposits its crystals. The complex flow field will determine how settling develops [34]. One may expect a marked contrast between crystals settling from a plume and from a lateral current sweeping across the floor.

Although it is not yet possible to make precise predictions of the size of plumes nor of crystal settling, the framework developed above has interesting implications.

5.1. The Upper Border Groups

At the top of magma chambers, one sometimes finds exactly the same crystallization sequence as at the bottom, only turned upside down and over a smaller thickness. This indicates that crystallization occurs from the roof downwards in the same manner than from the floor upwards. The roof sequence has been called the Upper Border Series in the Skaergaard. Other examples are found in the Lambertville sill [14] or in the Kiglapait intrusion [9]. In some igneous complexes, for example in the Bushveld, the Upper Border Group is not developed. This strange fact has received no explanation.

Consider the low-viscosity case which is relevant for all these complexes. If the magma temperature is high, we have shown that convective instability can occur before the onset of crystallization. In such a case, crystallization at the roof is impossible. As an extreme limit, one could even envisage roof melting with the chamber extending upwards [35]. At lower temperatures, this is no longer possible and part of the crystallized magma remains attached to the roof. This allows the preservation of an Upper Border Group. This roof sequence is of smaller thickness than that which forms at the floor, because the convective heat flux retards crystallization.

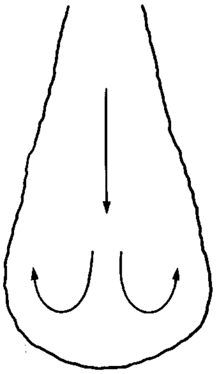

Fig. 11. Mean flow-field at the tip of a convective plume (from [33]). Note the inner circulation in the cap and the fuzzy edges of the plume where eddies entrain surrounding fluid.

5.2. Granites

As shown in Fig. 9, crystal-bearing plumes are not possible in magmas with viscosities exceeding 10^5 poise. This corresponds to the field of granites which rarely have igneous structures, and certainly lack the very complex structures of their basic or ultrabasic counterparts [5]. These observations suggest that there is more than a qualitative difference due to an increase of viscosity. We have shown that there is a difference of convection regime. In granites, thermal convection is weak and we expect bottom crystallization to be undisturbed by convective plumes coming from the top. Disturbances due to side-wall currents are possible, and have been recorded, as discussed below, but differ from those due to plumes.

5.3. Intermittent layering

We now apply our results to a specific petrological problem, the formation of intermittent layering, a particular form of rhythmic layering defined by McBirney and Noyes [6] in the Skaergaard intrusion. Because of the complexity of igneous layering, a few words are needed to clarify the issue.

Some of the most spectacular forms of layering have been observed in the ultramafic complex of Duke Island in Alaska [36]. Although not yet fully understood, these layered structures have been linked to the proximity of side walls. They usually show up as dipping layers with many characteristic features of sedimentary rocks: slumping, cross-bedding and discordant patterns [36]. Similar structures have been reported in almost all igneous bodies, including granites [5,37,38]. The generally accepted model is that they are due to the action of magmatic currents generated by side-wall cooling [7,39]. Such currents dominate in chambers of small aspect-ratio but are confined to the neighbourhood of the side walls in larger ones. We focus instead on intermittent layering, because McBirney and Noyes [6] have argued convincingly that it could not be due to wall currents. Specifically, intermittent layering consists of thin modally graded layers (typically 10 cm thick) alternating with layers of uniform rock of varying thickness (up to several meters) [5,6]. The thin modally graded layers usually occur in groups. This form of layering has also been found in the Stillwater [14], and Campbell has described very similar features in the Jimberlana intrusion [31]. The intriguing fact is that it is conspicuously absent from the Ultramafic Zone of the Stillwater [40], and also from granitic plutons [5]. The reason is not obvious, since it is now established that convection occurs in all these cases [3].

In basic and ultrabasic magmas, the regime of crystal-bearing plumes is likely. We suggest that it is at the origin of intermittent layering. Hess [14] and Wager and Brown [5] had recognized that this type of layering calls for a particular process operating only at occasional intervals. With crystal-bearing plumes, bottom crystallization proceeds both in-situ and by deposition from above. What is important is that the crystals coming from above are deposited as discrete batches and not continuously as they would be if they settled from a large reservoir. We thus expect the normal crystallization sequence to be perturbed occasionally. Also, we expect that, contrary to other forms of layering, due maybe to reinjection or oscillatory nucleation [2,5,41], the effects are of limited horizontal extent. Field observations show that intermittent layering is irregular and has a typical horizontal width of 200 m [14]. Geometrical relationships argue in favor of crystal deposition. McBirney and Noyes [6, p. 519] stated that "layering is commonly draped over the top of large blocks, and layered accumulations may fill narrow dike-like spaces between fragments of blocks that split on reaching the floor". Wager and Brown [5, p. 229] observed that the thin modally graded layers have adcumulate textures at their base which becomes more orthocumulate towards their top. The adcumulate texture is consistent with in-situ crystallization, and the orthocumulate one suggests conditions of faster accumulation consistent with deposition from above.

This model is only qualitative, but we have defined the conditions where it applies. Hence, it can be tested against several kinds of observations. First, the adcumulate textures which characterize the Ultramafic Zone of the Stillwater and the uniform rocks of the upper parts of the Skaergaard are remarkably similar [5]. Why then, is there no intermittent layering in the ultramafic zone in the Stillwater and why does it appear above? One answer could be that a compositional effect is involved, since intermittent layers include plagioclase crystals which are absent from the ultramafic zone. This explanation seems unlikely because of the peculiar deposition characteristics mentioned above. Further, plagioclase can be either at the bottom or at the top of the thin modally graded layers [6,14]. This is also true for a similar type of layering in the Jimberlana complex [31]. Intermittent layering develops with olivine, pyroxene and plagioclase crystals in the Skaergaard, and only pyroxene and plagioclase in the Stillwater. Therefore, it is not associated with any specific mineral sequence, and it is best described as a disturbance in the normal crystallization sequence developing at the bottom. Indeed, the thin graded layers do represent an anomaly in the general modal composition of the rocks [6]. We suggest the following model. During formation of the ultramafic zone of the Stillwater, in early stages of crystallization, temperatures were presumably the highest, especially if reinjection occurred. Hence, the regime of crystal-free plumes prevailed. Later in the chamber evolution, temperatures decreased, allowing a transition to the regime of crystal-bearing plumes and intermittent layering.

Second, we have shown that crystal-bearing plumes are not likely in granitic magmas, which accounts for the fact that intermittent layering has never been observed in these [5].

6. Conclusion

We have compared the characteristic time-scales of crystallization and thermal convection at the top of magma chambers. For small viscosity values (less than about 40 poise), convection develops before the onset of crystallization. Hence, crystal settling is unimportant because there is no time for crystals to grow. Furthermore, compositional differences cannot develop. At higher viscosity values, such as those for less mafic liquids, thermal instabilities develop in partly crystallized magma and crystal-bearing plumes are generated. At the bottom of the chamber, crystallization will thus proceed both in-situ and through intermittent deposition from the top. At viscosity values greater than about 10^5 poise, convection develops late and does not involve crystals. In a more general way, our results emphasize that the greater the magma viscosity, the smaller the temperature difference driving convection. One consequence is that thermal convection is weak in granites.

In basic complexes, intermittent layering is well-developed only in certain specific cases. We suggest that this depends on the interior temperature. If it is higher than the liquidus by more than 70°C, the plumes do not contain crystals. This regime prevailed during the formation of the Ultramafic Zone of the Stillwater. An interesting speculation is that, as the chamber cools, interior temperature decrease towards the liquidus, eventually drawing the system into the regime of crystal-bearing plumes. This explains why intermittent layering is observed at a later stage. The same alternative does not exist for granites which explains why they lack intermittent layering.

The story of thermal convection is essentially that of the top boundary layer at the roof. In contrast, the bottom boundary layer is stable and compositional effects develop that may eventually lead to density instabilities. These instabilities occur on a time-scale determined in part by that of crystallization, which is longer than that of thermal convection in basic magmas. This suggests that the layering of basic magma chambers develops on at least two different time and length scales.

Acknowledgements

Claude Allègre made valuable comments. We thank Stephen Tait, Ross Kerr, Bruce Marsh and S.A. Morse for helpful criticisms. We enjoyed fruitful discussions with Alexander McBirney, both in the office and on the outcrop. This is IPGP Contribution No. 885.

Appendix A—The kinetics of crystallization

1. The nucleation rate

In magmas, most nucleation probably occurs heterogeneously [30,42]. The factors which affect the nucleation rate are the same as for homogeneous nucleation, for which the theory is well known. The major difference lies in the critical temperature interval δT, called the nucleation delay, over which the nucleation rate is negligible [30]. The delay is small for silicate magmas. Using parameters suitable for heterogeneous nucleation and general expressions of homogeneous nucleation, we obtain an adequate expression for the nucleation rate. Following Turnbull [43–45], we take:

$$I = K_1 T \exp\left[-K_2/(T\theta^2)\right] . \exp(-K_3/T) \qquad \text{(A-1)}$$

where T is the absolute temperature and θ the undercooling $T_L - T$. K_1, K_2, and K_3 are set constant (Fig. A-1).

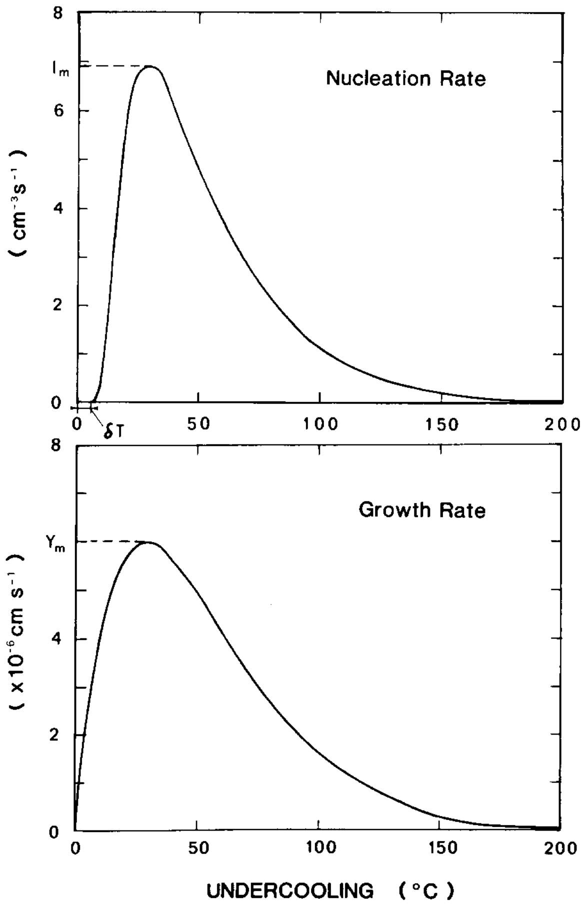

Fig. A-1. The functions used in this paper for the rates of nucleation and growth, versus undercooling ($\theta = T_L - T$).

2. The growth rate

In highly transient cooling conditions, crystal growth is controlled by the interface reactions [46] with a growth rate depending only on undercooling [47]. Chemical diffusion eventually becomes the limiting process [48,49]. We have shown that the controlling factor of crystallization is nucleation [20], and we take the simplest law for growth as a function of temperature only. Following Kirkpatrick [47], we write:

$$Y = K_4\left[1-\exp(-K_5\theta/T)\right]\exp(-K_6/T) \qquad \text{(A-2)}$$

where K_4, K_5 and K_6 are kept constant (Fig. A-1).

3. Numerical values

The values of parameters K_2, K_3 and K_5, K_6 are obtained with an adequate set of measurements in silicate melts (for more details see Dowty [30]). Data on nucleation rates [50,51] as well as on growth rates [30] have been taken into account to determine the values of K_1 and K_4. The nucleation and growth functions used in this paper are represented in Fig. A-1. We have taken $K_1 = 8\times10^{15}\ \text{cm}^{-3}\ \text{s}^{-1}\ \text{K}^{-1}$, $K_2 = 5\times10^5\ \text{K}^{-3}$, $K_3 = K_6 = 6\times10^4$ K, $K_4 = 2\times10^{13}$ cm/s, and $K_5 = 20$. Note that the nucleation delay is equal to $\simeq 5°\text{C}$, close to measured values in basaltic melts [52]. Table 1 gives the maximum values I_m and Y_m. Note that most crystallization takes place close to the liquidus, hence at rates much smaller than those maximum values ([20] and Fig. A-1).

4. Discussion

Because most of our analysis depends on these values, a few words are needed to clarify the assumptions and uncertainties.

The behavior of the nucleation rate at very slow cooling rates close to the liquidus cannot be studied in the laboratory conditions, but expression (A-1) allows us to predict likely values once the maximum is known. Using these functions, crystal sizes calculated in realistic conditions are in good agreement with petrological observations [20].

The same question arises for the growth rate. Several points are worth mentioning. First, some available laboratory data are in good agreement with the value selected. Second, we emphasize that data for both the nucleation and growth rates in the same system must be used. The values taken here are mutually consistent, as discussed in our earlier paper [20]. As already stated, they give good agreement with observed crystal sizes in many igneous rocks of all kinds, hence there is no basis for selecting widely differing values. Third, in a cooling experiment, what is important is the coupling between temperature and crystallization: the crystallization rate scales with (Y^3I) (equation 9c) which depends on temperature. Hence, the effective crystallization rate is determined not only by the kinetics but also by cooling regime. All else being equal, cases with different growth rate values Y_m also differ by their temperatures in the crystallizing region [20]. This explains why we find that the characteristic times for crystallization change little for various rates of nucleation and growth [20]. We found a range of one order of magnitude: from about 10^3 to 10^4 s. In comparison, viscosity values vary by more than 10^6, which leads to variations of more than 10^4 for the critical time of convection.

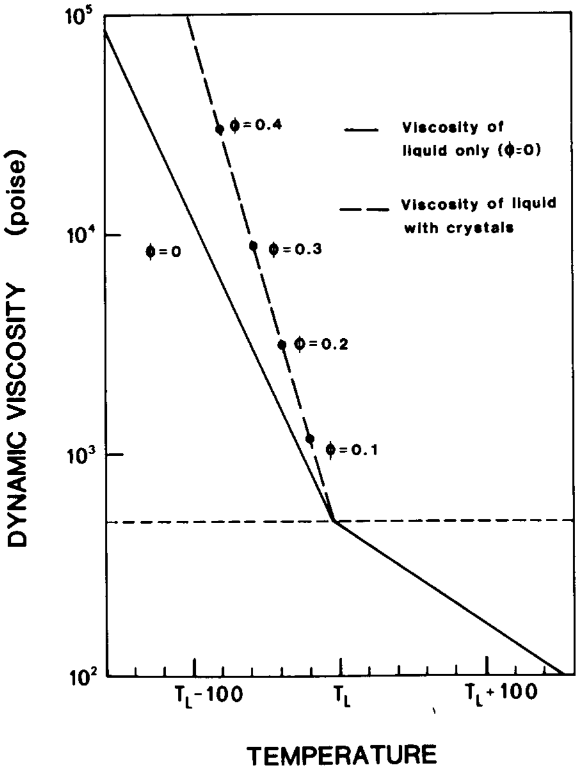

Fig. B-1. Viscosity function used in this paper. Solid curve: for liquid magma only. Dashed curve: for a suspension of magma and crystals (assuming that crystal content ϕ varies linearly with temperature). The kink at the liquidus is due to a change in activation energy. It has no effect on the numerical results of this paper.

However, it is clear that more data on rates of nucleation and growth are needed. We have derived a non-dimensional number C (equation 11a) which allows an easy evaluation of the effect of changing both Y_m and I_m.

We have neglected compositional effects. Our study allows for a crystallization interval of more than 200°C, as seen in Fig. A-1 where the rates of nucleation and growth are non-zero over a large temperature range. As discussed in [20] and for thermal reasons given at the end of section 3 (main text), crystallization takes place close to the liquidus over a rather thin region which advances into the magma. The consequences are that the crystallization temperature changes slowly and that the same phase nucleates and grows. This is observed in igneous complexes where almost monominerallic sequences are seen over thicknesses of more than 50 meters [5].

Appendix B—The viscosity of magmas

At temperatures above their liquidus, magmas are Newtonian and their viscosity depends on temperature according to an Arrhenius law [22]:

$$\mu = A \exp(E_0/RT) \tag{B-1}$$

where E_0 is the activation energy, R the gas content and T absolute temperature in Kelvin. Constant A depends on composition. E_0 varies between 30 and 180 kcal/mole, with a mean value of 50 kcal/mole [23,53].

Below the liquidus, our knowledge of the rheology of magmas is far from complete. For the liquid only, viscosity follows a law of the type:

$$\mu_1 = A \exp[E_1/R(T - T_2)] \tag{B-2}$$

where T_2 is the temperature of the glass transition [54]. The parameters in (B-2) are not well-known. Because we only need viscosity values at temperatures well above the glass transition, we shall consider an Arrhenius law with a different activation energy E_1. This is merely a convenient way of approximating (B-2) close to the liquidus. The ratio of liquid viscosities at the solidus and the liquidus, $\mu(\text{solidus})/\mu(\text{liquidus})$, is about 10^3 [23]. This corresponds to an activation energy of 135 kcal/mole for a crystallization interval of 200°C.

Below the liquidus, crystals start to grow and viscosity increases also as a function of crystal content. There may be Bingham behaviour with a finite yield strength [23,55]. However, the origin of this behaviour remains unclear [56] and we assume Newtonian rheology in agreement with most authors [2]. A yield strength would enhance the effects discussed in this paper. As a first approximation, the viscosity of a suspension depends only on ϕ, the crystal content. Up to ϕ values of 65%, a reasonable approximation is [57]:

$$\mu = \mu_1 \left(1 - \frac{\phi}{0.65}\right)^{-1.625} \tag{B-3}$$

μ_1 is the liquid viscosity with a temperature dependence described by (B-1). We fix both E_0 and E_1 at values of 50 and 135 kcal/mole respectively. Viscosity variations due to differences in composition are much more important than those due to variations of E_0 or E_1 and the simple law defined here is sufficient for our purposes. This law is depicted in Fig. B-1. Note that there is a kink at the liquidus, because the activation energy changes value. This has no effect on our results.

References

1 T.N. Irvine, Terminology for layered intrusions, J. Petrol. 23, 2, 127–162, 1982.

2 H.E. Huppert and R.S.J. Sparks, The fluid dynamics of a basaltic magma chamber replenished by influx of hot, dense ultrabasic magma, Contrib. Mineral. Petrol. 75, 279–289, 1980.

3 H.R. Shaw, Comments on viscosity, crystal settling, and convection in granitic magmas, Am. J. Sci. 263, 120–153, 1965.

4 R.W. Bartlett, Magma convection, temperature distribution and differentiation, Am. J. Sci. 267, 1067–1082, 1969.

5 L.R. Wager and G.M. Brown, Layered Igneous Rocks, 588 pp., Oliver and Boyd, Edinburgh, 1968.

6 A.R. McBirney and R.M. Noyes, Crystallization and layering of the Skaergaard intrusion, J. Petrol. 20, 487–554, 1979.

7 T.N. Irvine, Magmatic density currents and cumulus processes, Am. J. Sci. 280-A, 1–58, 1980.

8 C.F. Chen and J.S. Turner, Crystallization in a double-diffusive system, J. Geophys. Res. 85, 2573–2593, 1980.

9 S.A. Morse, The Kiglapait layered intrusion, Labrador, Geol. Soc. Am. Mem. 112, 1969.

10 H.E. Huppert and J.S. Turner, A laboratory model of replenished magma chamber, Earth Planet. Sci. Lett. 54, 144–152, 1981.

11 H.E. Huppert, R.S.J. Sparks and J.S. Turner, Laboratory investigations of viscous effects in replenished magma chambers, Earth Planet. Sci. Lett. 65, 377–381, 1983.

12 J.S. Turner, A fluid dynamical model of differential and layering in magma chambers, Nature 285, 213–215, 1980.

13 E.D. Jackson, Primary textures and mineral associations in the ultramafic zone of the Stillwater complex, Montana, Geol. Surv. Prof. Pap. 358, 106 pp., 1961.

14 H.H. Hess, Stillwater igneous complex, Geol. Soc. Am. Mem. 80, 230 pp., 1960.

15 R.H. Kraichnan, Turbulent thermal convection at arbitrary Prandtl number, Phys. Fluids 5, 1374–1389, 1962.

16 C. Jaupart, G. Brandeis and C.J. Allègre, Stagnant layers at the bottom of convecting magma chambers, Nature 308, 535–538, 1984.

17 L.N. Howard, Convection at high Rayleigh number, in: Proc. 11th Int. Congr. of Applied Mechanics, Munich, 1964, H. Görtler ed., pp. 1109–1115, Springer, Berlin, 1966.

18 C. Jaupart and B. Parsons, Convective instabilities in a variable viscosity fluid cooled from above, Phys. Earth Planet. Inter. 39, 14–32, 1985.

19 H. Williams and A.R. McBirney, Volcanology, 397 pp., Freeman Cooper, San Francisco, Calif., 1979.

20 G. Brandeis, C. Jaupart and C.J. Allègre, Nucleation, crystal growth and the thermal regime of cooling magmas, J. Geophys. Res. 89, 10161–10177, 1984.

21 R.J. Kirkpatrick, Towards a kinetic model for the crystallization of magma bodies, J. Geophys. Res. 81, 2565–2571, 1976.

22 H.R. Shaw, Rheology of basalt in the melting range, J. Petrol. 10, 510–535, 1969.

23 T. Murase and A.R. McBirney, Properties of some common igneous rocks and their melts at high temperature, Geol. Soc. Am. Bull. 84, 3563–3592, 1973.

24 C. Jaupart, On the mechanism of heat loss beneath continents and oceans, 215 pp., Ph.D. Thesis, MIT, Cambridge, Mass., 1981.

25 D.B. White, Experiments with convection in a variable viscosity fluid, Ph.D. Thesis, Cambridge University, 1982.

26 F.M. Richter, H.C. Nataf and S.F. Daly, Heat transfer and horizontally averaged temperature of convection with large viscosity variations, J. Fluid Mech. 129, 173–192, 1983.

27 D.A. Yuen and L. Fleitout, Stability of the oceanic lithosphere with variable viscosity: an initial value approach, Phys. Earth Planet. Inter. 34, 173–185, 1984.

28 G. Houseman, and D. McKenzie, Numerical experiments on the onset of convective instability in the Earth's mantle, Geophys. J.R. Astron. Soc. 68, 133–164, 1982.

29 S.A. Morse, Basalts and Phase Diagrams: An Introduction to the Quantitative Use of Phase Diagrams in Igneous Petrology, 493 pp., Springer, New York, N.Y., 1980.

30 E. Dowty, Crystal growth and nucleation theory and the numerical simulation of igneous crystallization, in: Physics of Magmatic Process, pp. 419–485, Princeton, University Press, Princeton, N.J., 1980.

31 I.H. Campbell, Some problems with the cumulus theory, Lithos 11, 311–323, 1978.

32 S.A. Morse, Thermal structure of crystallizing magma with two-phase convection, Geol. Mag., in press, 1986.

33 J.S. Turner, Buoyancy Effects in Fluids, Cambridge University Press, Cambridge, 1973.

34 B.D. Marsh and M.R. Maxey, On the distribution and separation of crystals in convecting magma, J. Volcanol. Geotherm. Res. 24, 95–150, 1985.

35 J.L. Ahern, D.L. Turcotte and E.R. Oxburgh, On the upward migration of an intrusion, J. Geol. 89, 421–432, 1981.

36 T.N. Irvine, Petrology of the Duke Island ultramafic complex, southeastern Alaska, Geol. Soc. Am. Mem. 138, 1974.

37 T.E. Smith, Layered granitic rocks at Chebucto Head, Halifax Country, Nova Scotia, Can. J. Earth Sci. 12, 456–463, 1975.

38 M. Barriere, On curved laminae, graded layers, convection currents and dynamic crystal sorting in the Ploumanac'h (Brittany) subalkaline granite, Contrib. Mineral. Petrol. 77, 214–224, 1981.

39 F. Spera, D.A. Yuen and S.J. Kirschvink, Thermal boundary layer convection in silicic magma chambers: effects of temperature-dependent rheology and implications for thermogravitational chemical fractionation, J. Geophys. Res. 87, 8755–8767, 1982.

40 E.D. Jackson, The origin of ultramafic rocks by cumulus processes, Fortschr. Mineral. 48, 128–174, 1971.

41 S.R. Tait, Fluid dynamical and geochemical evolution of cyclic unit 10, Rhum, Eastern Layered Series, Geol. Mag. 122, 469–484, 1985.

42 R.J. Kirkpatrick, Nucleation and growth of plagioclase, Makaopuhi and Alae lava lakes, Kilauea Volcano, Hawaii, Geol. Soc. Am. Bull. 88, 78–84, 1977.

43 D. Turnbull and J.C. Fisher, Rate of nucleation in condensed systems, J. Chem. Phys. 17, 71–73, 1949.

44 D. Turnbull, Formation of crystal nuclei in liquid metals, J. Appl. Phys. 21, 1022–1028, 1950.

45 D. Turnbull, Kinetics of solidification of supercooled liquid mercury droplets, J. Chem. Phys. 20, 411–424, 1952.

46 C.J. Allègre, A. Provost and C. Jaupart, Oscillatory zoning: a pathological case of crystal growth, Nature 294, 223–228, 1981.

47 R.J. Kirkpatrick, Crystal growth from the melt: a review, Am. Mineral. 60, 798–814, 1975.

48 A.C. Lasaga, Towards a master equation in crystal growth, Am. J. Sci. 282, 1264–1320, 1982.

49 T.P. Loomis, Numerical simulations of crystallization processes of plagioclase in complex melts: the origin of major and oscillatory zoning in plagioclase, Contr. Mineral. Petrol. 81, 219–229, 1982.

50 S.E. Swanson, Relation of nucleation and crystal-growth rate to the development of granitic textures, Am. Mineral. 62, 966–978, 1977.

51 P.H. Fenn, The nucleation and growth of alkali feldspars from hydrous melts, Can. Mineral. 15, 135–161, 1977.

52 C.H. Donaldson, An experimental investigation of the delay in nucleation of olivine in mafic magmas, Contrib. Mineral. Petrol. 69, 21–32, 1979.

53 Y. Bottinga and D.F. Weill, The viscosity of magmatic silicate liquids: a model for calculation, Am. J. Sci. 272, 438–475, 1972.

54 P. Richet, Propriétés thermodynamiques des silicates fondus, Thèse d'état, Paris, 1982.

55 H.R. Shaw, T.L. Wright, D.L. Peck and R. Okamura, The viscosity of basaltic magma: an analysis of field measurements in Makaopuhi Lava lake, Hawaii, Am. J. Sci. 266, 225–264, 1968.

56 R.S.J. Sparks and H. Pinkerton, Effect of degassing on rheology of basaltic lava, Nature 276, 385–386, 1978.

57 D.J. Jeffrey and A. Acrivos, The rheological properties of suspensions of rigid particles, Am. Inst. Chem. Eng. J. 22, 3, 417–432, 1976.